Structural Studies of the Contractile Tail Sheath Protein of Bacteriophage T4. 2. Structural Analyses of the Tail Sheath Protein, Gp18, by Limited Proteolysis, Immunoblotting, and Immunoelectron Microscopy†

Fumio Arisaka,* Shigeki Takeda, Kazue Funane, Noriko Nishijima, and Shin-ichi Ishii
Department of Biochemistry, Faculty of Pharmaceutical Sciences, Hokkaido University, Sapporo, Japan 060
Received August 10, 1989; Revised Manuscript Received November 28, 1989

ABSTRACT: The molecular structure of the T4 phage tail sheath protein, gp18, was studied by limited proteolysis, immunoblotting, and immunoelectron microscopy. Gp18 is extremely resistant to proteolysis in the assembled form of either extended or contracted sheaths, but it is readily cleaved by proteases in the monomeric form, giving rise to stable protease–resistant fragments. Limited proteolysis with trypsin gave rise to a trypsin-resistant fragment, Ala82–Lys316, with a molecular weight of 27K. Chymotrypsin- and thermolysin-resistant fragments were also mapped close to the trypsin-resistant region. The time course of trypsin digestion of the monomeric gp18 as monitored by SDS–polyacrylamide gel electrophoresis and immunoblotting of the gel revealed that the polypeptide chain consisting of 658 amino acid residues is sequentially cleaved at several positions from the C terminus. The N-terminal portion, Thr1–Arg81, was then removed to form the trypsin-resistant fragment. Immunoelectron microscopy revealed that the polyclonal antibodies against the trypsin-resistant fragment bound to the tail sheath. This supported the idea that at least part of the protease-resistant region of gp18 constitutes the protruding part of the sheath protein as previously revealed with three-dimensional image reconstruction from electron micrographs by Amos and Klug [Amos, L. A., & Klug, A. (1975) *J. Mol. Biol. 99*, 51–73].

Bacteriophage T4 and related phages have a long contractile tail, which is an elaborate organelle to ensure high efficiency of infection. The tail consists of two parts, namely, the long cocylindrical part and the baseplate attached to the distal end. In contrast with the complex structure and the number of components of the baseplate, the cocylindrical part has a relatively simple structure. Both inner and outer cylinders consist of 144 promoters of tube and sheath proteins (gp19 and gp18; gp, gene product), respectively (Moody, 1973). Upon adsorption of the phage to the bacterium, the conformational change of the baseplate from "hexagon" to "star" triggers contraction of the sheath. The inner tube then protrudes from the bottom of the baseplate and penetrates into the outer membrane (Simon & Anderson, 1967). The genomic phage DNA packaged in the head is then ejected through the tube into the periplasm of the bacterium.

The structure of the sheath in the extended and contracted forms has been studied by a number of authors with electron microscopy (Kellenberger & Boy de la Tour, 1965; Moody, 1967; Amos & Klug, 1975; Smith et al., 1976; Lepault & Leonard, 1985). Moody investigated the lattice transformation of the tail sheath from the extended to contracted states by examining incompletely contracted sheaths which had been partially fixed with formaldehyde (Moody, 1973). The results indicated that the lattice transformation initiates at the baseplate and is propagated like a wave all the way to the proximal end of the sheath. During the lattice transformation, the sheath increases its diameter from 20 to 25 nm and decreases its length from 95 to 38 nm in such a way that the bonds between gp18 protomers in each annulus are disconnected and each protomer molecule slides into two adjacent protomer molecules in the neighboring annulus to form much stronger contacts (Amos & Klug, 1975). There is no covalent modification in the sheath protein upon contraction (Yamamoto & Uchida, 1975). Contraction is irreversible and occurs spontaneously without energy when triggered by the conformational change of baseplates: the extended sheath is considered to be a metastable structure.

Further elucidation of the mechanism of contraction requires knowledge of more detailed structure of the tail sheath protein, gp18. The accompanying paper describes structural studies by chemical modifications. In this paper, we describe the results from limited proteolysis, immunoblotting, and immunoelectron microscopy.

Materials and Methods

Enzymes and Reagents. Deoxyribonuclease I, trypsin (bovine pancreas), and chymotrypsin were purchased from Sigma Chemical Co. Lysyl endopeptidase was purchased from Wako Jun-yaku Co., and thermolysin was purchased from Seikagaku-kogyo Co. Trypsin purchased from Sigman was further purified by affinity chromatography (Kumazaki et al., 1986) and treated with L-1-(tosylamino)-2-phenylethyl chloromethyl ketone (TPCK). Protein A–gold complex (GP-01-5; solution) was purchased from EY Laboratories Co. All other reagents were of analytical grade from Nakarai Chemicals or Wako Jun-yaku. Nutrient broth, bactotryptone, yeast extract, bactoagar, and casamino acids were purchased from DIFCO Laboratories. Protein A–Cellulofine was a product of Seikagaku-kogyo Co.

Media and Buffer. SDS[1] sample buffer (three times concentrated) contained 15 mL of glycerol, 7.5 mL of 2-mercaptoethanol, 3.45 g of SDS, and 1.14 g of Tris base in

† This work was supported by Grant-in-Aids for Scientific Research from the Ministry of Education, Science, and Culture of Japan.

* Address correspondence of this author at his present address: Department of Life Science, Tokyo Institute of Technology, 4259 Nagatsuta, Midori-ku, Yokohama, Japan 227.

[1] Abbreviations: ELISA, enzyme-linked immunosorbent assay; HPLC, high-performance liquid chromatography; IgG, immunoglobulin; Tris, tris(hydroxymethyl)aminomethane; SDS, sodium dodecyl sulfate.

0006-2960/90/0429-5057$02.50/0

a 50-mL solution; the pH was adjusted to 6.8 with concentrated HCl. All other media and buffers used in this study are described in the accompanying paper (Takeda et al., 1990).

Phage and Bacterial Strains. T4D wild-type phage and T4D.23amH11 are from our collection. *Escherichia coli* BE was used as a nonpermissive host for amber mutant phages, and *E. coli* CR63 was the permissive host.

Preparation of Tails and Gp18. Tails and gp18 were prepared according to the method of Tschopp et al. [1979; see also Takeda et al. (1990)].

Purification of Phage Particles. T4D phage particles for immunoelectron microscopy were purified by CsCl step gradient centrifugation (Dickson, 1974).

SDS–Polyacrylamide Gel Electrophoresis. SDS gel electrophoresis was carried out according to the buffer system of Laemmli (1970). Slab gels, 7.5 cm × 9 cm × 1 mm, were used for analytical purposes. For preparative purposes, a gel size of 12 cm × 14 cm × 5 mm (or 2 mm) was used.

Limited Proteolysis of Gp18. Stock solutions of proteases for limited proteolysis were prepared as follows: trypsin, 0.31 mg/mL in 1 mM HCl; chymotrypsin, 0.19 mg/mL in 1 mM HCl; lysyl endopeptidase, 0.15 mg/mL in 5 mM Tris·HCl, pH 8.0; thermolysin, 0.5 mg/mL in 10 mM Tris·HCl–10 mM $CaCl_2$, pH 8.0. Protease was added in the weight ratio of 1/100 to 100 μL of native monomeric gp18 solution (0.2 mg/mL) in 1 mM phosphate buffer, pH 7.2 and incubated at 30 °C. Ten microliters of the reaction mixture was withdrawn with time intervals as indicated in legends to Figure 1 to monitor digestion. Five microliters of SDS sample buffer (3× concentrated) was immediately added to each withdrawn sample solution, and the reaction was stopped by heating in boiling water for 3 min. The sample was then loaded on SDS gel for electrophoresis.

Isolation of Protease-Resistant Fragments from SDS Gel. Approximately 2 mg of native monomeric gp18 was digested with 0.02 mg of a protease at 30 °C for sufficient time for producing protease-resistant fragments (see above). Digestion was stopped by SDS addition and heat treatment as described above, and the digest was loaded on SDS gel for electrophoresis. Sodium thioglycolate (final concentration of 0.1 mM) was added to the cathode buffer reservoir (Hunkapiller et al., 1983). After slight staining with Coomassie brilliant blue R250, the desired band was cut out with a razor blade and the fragment was electrophoretically extracted with an ISCO concentrater (Model 1750) by using the same SDS electrophoresis buffer. The extracted fragments were dialyzed once against 0.2 M NaCl and then extensively dialyzed against water (MilliQ grade was used).

Sequence Determination of Peptides. N-Terminal amino acid sequences of protease-resistant fragments were determined on a pulsed liquid protein sequencer, Applied Biosystems 477A. Usually, 0.5–1 nmol of sample was subjected to analysis. PTH amino acids were identified by high-performance liquid chromatography (HPLC).

Preparation of Anti-Sera Against Gp18 and Its Fragments. Gp18 and the trypsin-resistant fragment were prepared as described above. The N-terminal fragment, Thr1–Val14, was synthesized by an Applied Biosystems 430A peptide synthesizer by using the standard manufacturer's protocol (single couplings). Trifluoromethanesulfonic acid was used as a cleavage/deprotection reagent, and the deprotected peptide was purified by reverse-phase HPLC. The C-terminal fragment, Ala596–Gly658 (K-30), was isolated by reverse-phase HPLC as described in the accompanying paper (Takeda et al., 1990).

Approximately 0.2 mg of gp18 in 0.5 mL was mixed with 0.5 mL of Freund's complete adjuvant and injected on the back of a rabbit three times at 1-week intervals. One-tenth milligram of trypsin-resistant fragment was also used as antigen and injected to a rabbit in the same way. For the C-terminal fragment, a total of 50 pmol was used as antigen. The N-terminal fragment was coupled to hemocyanin from *Helix pomatia* as a carrier protein by 1-ethyl-3-[3-(dimethylamino)propyl]carbodiimide hydrochloride. Amino acid analysis of the peptide-bound hemocyanin showed that 27.4 molecules of the peptide bound to one subunit of hemocyanin. One milligram of the peptide-bound hemocyanin was injected to a rabbit as described above three times. One milligram of the peptide-bound hemocyanin plus 1.5 mg of the free peptide and 1.5 mg of the free peptide alone were injected as fourth and fifth immunizations, respectively, and the antibodies were finally detected.

Production of antibodies were checked by immunoblotting of SDS gels of tail proteins as described below.

Immunoblotting. After electrophoresis, proteins were transferred from SDS–polyacrylamide gels to nitrocellulose paper, and antigens were detected with unlabeled antibodies and an enzyme-linked detection system using a commercial immunohistochemical staining kit (Vector Laboratories, Burlingame, CA, No. PK 4001) according to the method of Duda et al. (1986).

Purification of IgG Fractions. IgG fractions were affinity-purified with protein A–Cellulofine. Ten milliliters of washing buffer (0.1 M sodium phosphate buffer, pH 7.0) was added to the same volume of anti-serum, and the mixture was applied to 5 mL of protein A–Cellulofine column. After the column was washed with 25 mL of the buffer, IgG's were eluted with 0.1 M glycine hydrochloride, pH 3.0. The eluates (2-mL fractions) were immediately neutralized with 0.5 mL of 0.2 M sodium phosphate buffer, pH 8.5.

Immunoelectron Microscopy. Samples were applied to carbon-coated collodion films on 200-mesh grids that had been rendered hydrophilic by glow discharge and were negatively stained with 1% uranyl acetate. Specimens were examined in a HITACHI 12A electron microscope. When protein A–gold was used, samples were first applied to the grid described above and rinsed with 3 drops of water at 30-s intervals. The background was then coated with bovine serum albumin by applying 1 drop of 20 mg/mL of the protein. After the samples were rinsed with water three times, unlabeled IgG was applied to the samples, and protein A–gold which had been diluted 10 times was bound to the IgG. Specimens were then negatively stained and observed in an electron microscope.

When a sample was mixed with antibodies in solution, unbound antibodies were removed by gel filtration through a Sepharose 6B column (7 mL in a 10-mL pipet) before application of the mixture to a grid.

Results

Limited Proteolysis of Monomeric Gp18. Limited proteolysis was used as a probe for structural studies of gp18. Gp18 is highly resistant to proteolysis when assembled into either extended or contracted sheath. Monomeric gp18, however, is susceptible to proteases and gives rise to protease-resistant fragments via several cleavage intermediates (Figure 1). Trypsin, chymotrypsin, and thermolysin gave rise to protease-resistant fragments having molecular weights of 27K, 29K, and 26K, respectively. In the case of lysyl endopeptidase, both 42K and 31K protease-resistant fragments were produced. Those protease-resistant fragments were extracted from the SDS gel, and each of their 20 N-terminal

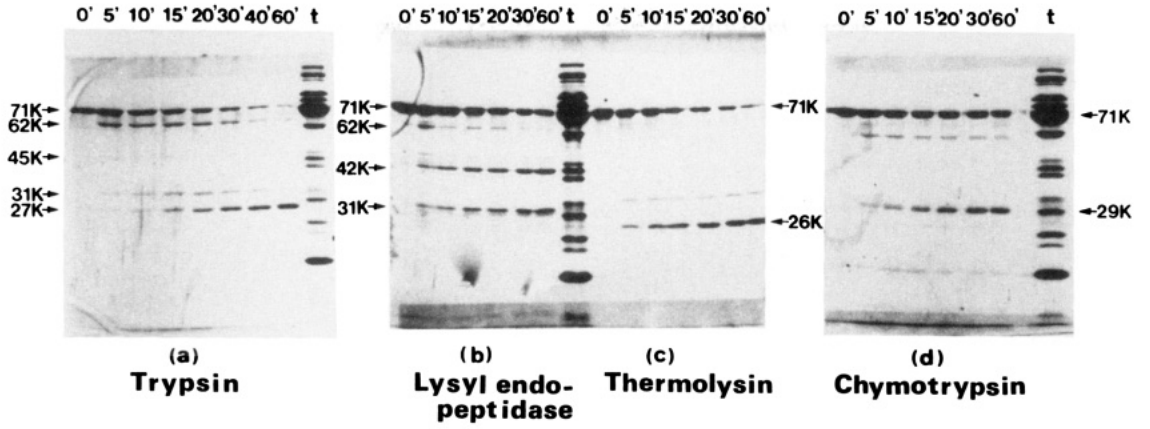

FIGURE 1: Limited proteolysis of gp18 by (a) trypsin, (b) lysyl endopeptidase, (c) thermolysin, and (d) chymotrypsin. Native monomeric gp18 was digested by each protease, and the time course of digestion was monitored by SDS–polyacrylamide gel electrophoresis. Except for lysyl endopeptidase, all the proteases gave rise to one protease-resistant fragment. Lysyl endopeptidase produced two stable fragments.

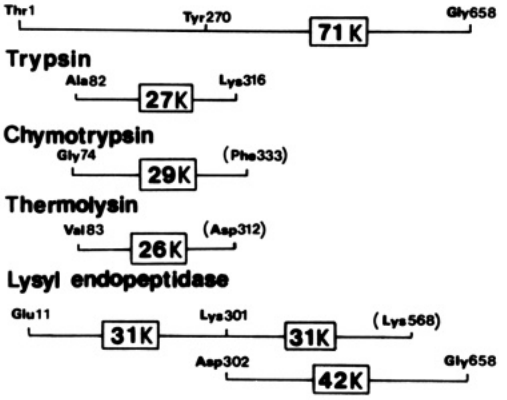

FIGURE 2: Mapping of protease-resistant fragments on the primary structure. Each protease-resistant fragment was isolated from SDS gel, and the N-terminal sequences were determined by a protein sequencer. Except for trypsin-resistant fragments, where the peptide map was also examined, C-terminal positions were inferred from the molecular weights and the residue specificity of each enzyme. For example, thermolysin-resistant fragment was assigned to the product by cleavages at Ala82–Val83 and Asp312–Phe313. The location of Tyr270, which is modifiable with tetranitromethane independent of the association state of gp18, is shown as a reference.

residues was sequenced. For the trypsin-resistant 27K fragments, peptide mapping with lysyl endopeptidase was also carried out (results not shown). For other protease-resistant fragments, C termini were inferred from their molecular weights and the specificities of proteases. The results are shown in Figure 2. The trypsin-, chymotrypsin-, and thermolysin-resistant fragments were Ala82–Lys316, Gly74–Phe333, and Val83-Asp312, respectively.

On the other hand, the 42K fragment by lysyl endopeptidase was Asp302–Gly658. The 31K fragment by this protease turned out to be a mixture of Glu11–Lys301 and Asp302–Lys568, the former being the major species. Apparently, the 42K fragment slowly converts into 31K (Asp302–Lys568) which comigrates with Glu11–Lys301 in the SDS gel electrophoresis (see Figure 1). It is likely that lysyl endopeptidase makes only nicks in gp18, and the resultant two large fragments are not dissociated from each other, because when 5 mM $MgSO_4$ was added to the gp18 solution after treatment with lysyl endopeptidase, the cleavage product forms a polysheath-related structure that appears to be very fragile (Figure 3). Gel permeation chromatography of the lysyl endopeptidase digests of gp18 supports this interpretation; no smaller fragment than the whole gp18 molecule is detected (data not shown). Except for the lysyl endopeptidase digestion, all protease-resistant fragments were mapped in the N-terminal

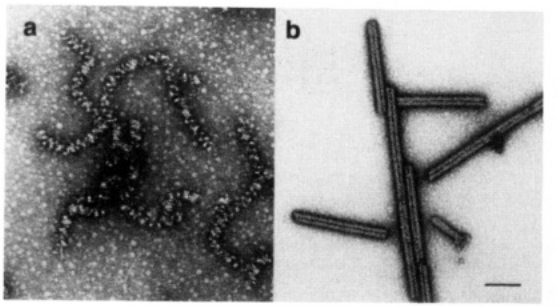

FIGURE 3: (a) Polysheath-related structure formed after cleavage with lysyl endopeptidase and addition of 5 mM $MgSO_4$ and (b) normal polysheaths. Normal polysheath was made from gp18 by addition of 5 mM $MgSO_4$. Bar, 100 nm.

half of the gp18 molecule. The C-terminal half of gp18 is resistant to lysyl endopeptidase presumably because the enzyme has the highest substrate specificity among those used in this experiment.

Analyses of Cleavage Intermediates by Immunoblotting. Cleavage intermediates by trypsin were analyzed by immunoblotting of the SDS gels. The identical SDS gels for typsin and lysyl endopeptidase digestion as shown in Figure 1 were blotted onto a nitrocellulose filter and immunostained as described under Materials and Methods (Figure 4). All intermediates for trypsin cleavage were stained when anti-trypsin-resistant fragment antiserum was used (Figure 4a). On the other hand, only whole gp18, which remained uncleaved, was detected when anti-C-terminal peptide antiserum was used. This indicated that the largest fragment, 62K, had already lost the C-terminal part of gp18. When anti-N-terminal peptide antiserum was used, all the intermediates except for the 27K fragment were stained (data not shown). In the case of lysyl endopeptidase digestion, anti-C-terminal peptide antibodies bound to the 42K fragment, but not to the 31K fragment, indicating that the 42K fragment contained the C-terminal fragment. The above results are consistent with the interpretation of the cleavage pattern depicted in Figure 5. It indicates that trypsin cleaves gp18 at a number of sites sequentially from the C terminus and finally cleaves at the peptide bond between Arg81 and Ala82 to produce the trypsin-resistant fragment.

Immunoelectron Microscopic Observations. IgG fractions were purified by protein A–Cellulofine column chromatography from the four kinds of antisera described above (i.e., anti-gp18, anti-trypsin-resistant fragment, anti-N-terminal, and anti-C-terminal) and used for immunoelectron microscopy. All these polyclonal antibodies appeared to contain antibody

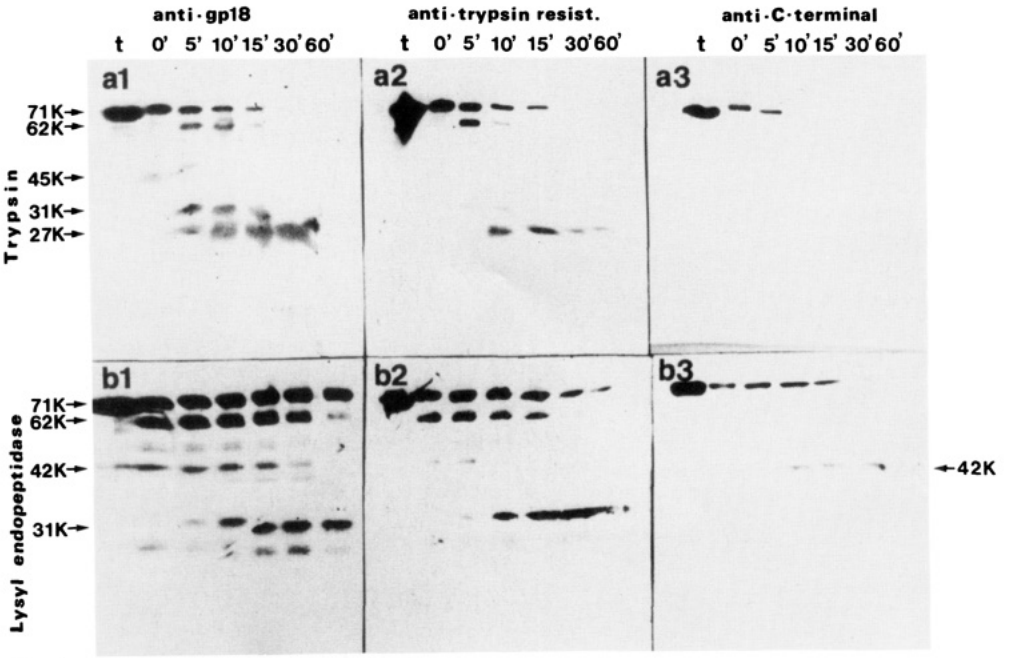

FIGURE 4: Immunoblotting of (a1–3) trypsin-digested and (b1–3) lysyl endopeptidase digested gp18. (a1), (b1), Anti-gp18 antiserum; (a2), (b2), anti-trypsin-resistant-fragment antiserum; (a3), (b3), anti-C-terminal peptide antiserum. SDS gels made under conditions identical with those of Figure 1 were used.

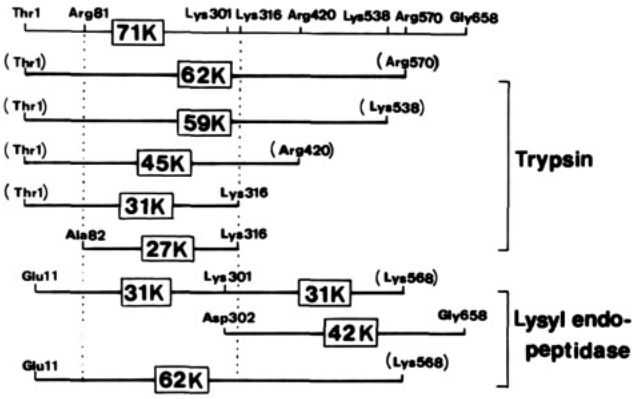

FIGURE 5: Cleavage intermediates of gp18 by trypsin and lysyl endopeptidase. C-Terminal residues which are in parentheses are those only inferred from the molecular weight of the intermediate and the specificities of the enzyme.

species which bind to native gp18 judged from the fact that the antibodies were detected by ELISA on a 96-hole titer plate, where gp18 was attached to the bottom of the holes under conditions where gp18 is expected to be in the native monomeric form.

Two methods were adopted. In the first method, phage particles or tails were first adsorbed on the grid and treated with antibodies. Protein A–colloidal gold was then applied. In the second method, antibodies and samples were first mixed in solution. The complexes freed from unadsorbed antibodies by gel filtration were then adsorbed on the grid and observed with an electron microscope (see Materials and Methods for details). The results are shown in Figure 6. When anti-gp18 antibodies or anti-trypsin-resistant fragment antibodies were used, they specifically bound to the tail sheaths (Figure 6a). They could also bind to the polysheath and contracted sheath (data not shown). When the second method was applied with the same antigen–antibody system, most phage particles were found to adhere to another phage particle at the tail sheath (Figure 6b). The anti-C-terminal antibodies did not bind to the tail sheath. Occasional binding of anti-N-terminal antibodies was observed as examined by protein A–gold, but the

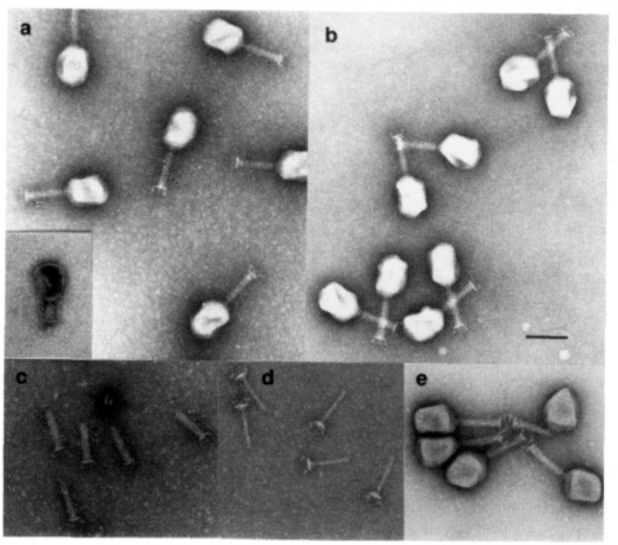

FIGURE 6: Immunoelectron microscopy. (a) Phage particles were treated with anti-trypsin-resistant fragment antibodies on the grid, binding of antibodies was visualized with protein A–gold. (b) Phage particles were treated with anti-trypsin-resistant antibodies in solution; the same images were obtained for phage particles with anti-gp18 antibodies. The insert in (a) shows that the antibodies bound to contracted sheath as well. (c) Tails were reacted with anti-trypsin-resistant fragment antibodies and protein A–gold. (d) Tails were incubated with anti-gp18 antibodies. (e) Phage particles were incubated with anti-N-terminal peptide antibodies. Bar, 100 nm.

binding appeared to be weak. Tails were also treated with anti-trypsin-resistant fragment antibodies with the first method, and the same results were obtained (Figure 6c). However, when the second method was used with antibodies against whole gp18 molecule, only tube–baseplates deprived of gp18 were detected (Figure 6d). Apparently, gp18 was dissociated from the tails and bound to the antibodies. This is reasonable if one considers that the polyclonal antibodies should contain antibody species that bind to the interacting regions of the molecular surface of gp18 in the tail sheath.

Unexpected results were obtained when phage particles and antibodies against N-terminal peptide were mixed in solution

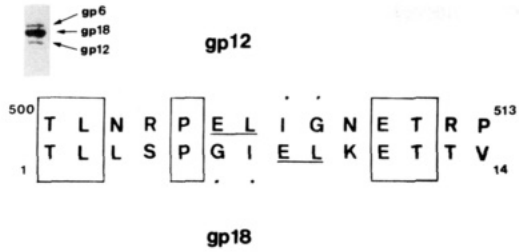

FIGURE 7: Local sequence similarity between the N-terminal peptide of gp18 and the C-terminal region of gp12. (Insert) Immunoblotting of tail proteins detected with anti-N-terminal peptide antibodies.

and then observed with an electron microscope. In this case, phage particles had a tendency to associate at the peripheral region of the baseplates (Figure 6e). Since antibodies were raised against a synthetic peptide, it is not likely that the antigen was contaminated with other tail components. A closer examination of the immunoblotting has shown that the antibodies cross-reacted with gp6 and gp12 (Figure 7, insert). It was, therefore, suspected that these proteins have partial sequence homology. The amino acid sequence of gp6 is not available as of July 1989; the protein is thought to be a baseplate component that is presumably located in the inner part of the baseplate (Watts & Coombs, 1989). On the other hand, a sequence similar to the N-terminal fragment was found in the C-terminal part of gp12 (Selivanov et al., 1989) as shown in Figure 7. We postulate that the anti-N-terminal peptide antibodies recognized the C-terminal part of gp12.

Discussion

Among phage constituent proteins, gp18, the tail sheath protein of phage T4, provides an exceptional opportunity to elucidate the structural feature controlling its assembly modes in that it can be analyzed in three assembly states, namely, extended sheath state, contracted sheath state, and native monomeric form. Making use of this advantage, we have investigated the molecular nature and structure of gp18 by limited proteolysis, immunoblotting immunoelectron microscopy, and chemical modification; the results of the former study are reported in this paper and those of the latter in the accompanying paper (Takeda et al., 1990).

Limited proteolysis and immunoblotting analyses have revealed that gp18 can be cleaved only in a monomeric form. In the case of trypsin, it is sequentially cleaved at a number of sites in the C-terminal half of gp18 from the C-terminal region, and then the N-terminal region, Thr1–Arg81, was removed to give rise to a protease-resistant fragment. Since the first cleavage may well affect the conformation of the molecule, we cannot argue that the second and later cleavage sites are also located on the surface of the molecule. However, the fact that distribution of these cleavage sites coincided well with that of chemically modifiable tyrosine residues [see Figure 4 of the accompanying paper, Takeda et al. (1990)] strongly indicates that the cleavable sites in the C-terminal half are most accessible from surroundings than those in the other half, especially in the protease-resistant region, of the gp18 monomer molecule. This appears to be reflected in the experimental result showing that the gp18 monomer undergoes reversible three-state conversion in guanidine hydrochloride denaturation and in thermal denaturation in alkaline pH; that is, gp18 consists of at least two domains (Arisaka, Yutani, and Ishii, unpublished experiments).

Immunoelectron microscopy has revealed that the trypsin-resistant fragment contains an epitope which is exposed to the solvent in the tail sheath. This is in agreement with our working hypothesis that the protease-resistant fragment constitutes the protruding part of the sheath structure as revealed by three-dimensional image reconstruction from electron micrographs (Amos & Klug, 1975). It is noted that the protease-resistant fragment contains Tyr270, which is modified with tetranitromethane independent of the association state of gp18 (Takeda et al., 1990). Residues near the C terminus of gp18 do not seem to be exposed on the surface of the sheath structure since anti-C-terminal fragment antibodies did not bind to the tail. The N-terminal part may be exposed on the surface of the sheath structure since occasional binding of anti-N-terminal peptide antibodies to the tail sheath was observed, but apparently the binding was not very strong.

To assist in the structural analysis of gp18, we have recently determined the nucleotide sequence of the contractile tail sheath gene of *Pseudomonas aeruginosa* phage PS17 (Sasaki, Shinomiya, Arisaka, and Ishii, unpublished results). It consisted of 384 amino acids. The sequence similarity between gp18 and the tail sheath protein from phage PS17 was unexpectedly low, but the computer analysis of similarity has revealed that the corresponding sequence of PS17 tail sheath protein in gp18 (ca. 20% identical) is split into two parts and is present in two separate places. Many phage species are known to possess contractile tail sheath, but the molecular weight varies to a great extent from 40K in the smallest (PS17 phage) to 71K in the largest (T4 phage) [see Arisaka et al. (1988)]. Further comparisons of primary structures of the contractile sheath proteins will give insights on the structural elements that are necessary for contraction as well as morphogenesis of the tail sheath.

Another attractive feature of the tail sheath protein is the availability of mutants. Five phenotypes of mutations in gene 18 are known, namely, amber (am), temperature sensitive (ts), cold sensitive (cs), heat sensitive (hs), and polyethylene glycol resistant (CBW) mutants [see Arisaka et al. (1988)]. As a next step toward elucidation of the structure–function relationship, we are currently analyzing the mutation sites of these mutants.

Acknowledgments

We thank Professor Edward Goldberg for invaluable comments on the manuscripts. We also thank Dr. Robert Duda for introducing F.A. to immunoblotting and immunoelectron microscopy. F.A. also thanks Professor F. A. Eiserling for valuable discussions and hospitality during his visit at UCLA, where he learned these techniques.

References

Amos, L. A., & Klug, A. (1975) *J. Mol. Biol. 99*, 51–73.
Arisaka, F., Nakako, T., Takahashi, H., & Ishii, S. (1988) *J. Virol. 62*, 1186–1193.
Dickson, R. C. (1974) *Virology 59*, 123–138.
Duda, R. L., Gingery, M., & Eiserling, F. A. (1986) *Virology 151*, 296–314.
Hunkapiller, M. W., Lujan, E., Ostrander, F., & Hood, L. E. (1983) *Methods Enzymol. 911*, 227–236.
Kellenberger, E., & Boy de la Tour, E. (1964) *J. Ultrastruct. Res. 11*, 545–563.
Laemmli, U. K. (1970) *Nature 227*, 680–685.
Lepault, J., & Leonard, K. (1985) *J. Mol. Biol. 182*, 431–443.
Moody, M. F. (1967) *J. Mol. Biol. 25*, 201–208.
Moody, M. F. (1973) *J. Mol. Biol. 30*, 613–635.
Selivanov, N. A., Prilipov, A. G., & Mesyanzhinov, V. V. (1989) *Nucleic Acids Res. 16*, 2334.
Simon, L. D., & Anderson, T. F. (1967) *Virology 32*, 298–305.
Smith, P. R., Aebi, U., Josephs, R., & Kessel, M. (1976) *J. Mol. Biol. 106*, 243–275.

Takeda, S., Arisaka, F., Ishii, S., & Kyogoku, Y. (1990) *Biochemistry* (preceding paper in this issue).
Tschopp, J., Arisaka, F., van Driel, R., & Engel, J. (1979) *J. Mol. Biol. 128*, 281–286.
Watts, N. R. M., & Coombs, D. H. (1989) *J. Virol. 63*, 2427–2436.
Yamamoto, M., & Uchida, H. (1975) *J. Mol. Biol. 92*, 207–223.

A Comparative Study of the Unfolding Thermodynamics of Vertebrate Metmyoglobins†

Lenore Kelly‡ and Leslie A. Holladay*,§
Department of Chemistry, Louisiana Tech University, Ruston, Louisiana 71272
Received September 25, 1989; Revised Manuscript Received January 24, 1990

ABSTRACT: Differential scanning microcalorimetry (DSC) of horse, rat, opossum, raccoon, carp, and armadillo metmyoglobins at alkaline pH gave data that fit the two-state unfolding model well. Monte Carlo studies were used to assess the impact of truncating DSC scans on the reliability of the calculated results when aggregation exotherms overlapped the unfolding endotherm at the high-temperature end of the scan. The DSC estimates for the conformational free energy at pH 8 and 298 K are compared to earlier results from isothermal acid and guanidinium chloride unfolding. Stability estimates at pH 8 for these six metmyoglobins obtained by DSC experiments do not agree with free energy estimates at pH 8 from guanidinium chloride unfolding. This is true for all three models used to extrapolate the free energy change to 0 M guanidinium chloride. Among these six myoglobins, significant variation appears in the temperature at which the myoglobin is half-unfolded, in the change in heat capacity upon unfolding, and in the change in enthalpy at 310 K. Calculations made with the hydrophobic model for protein folding [Baldwin, R. L. (1986) *Proc. Natl. Acad. Sci. U.S.A. 83*, 8069] suggest that a sizable variation exists for that portion of the unfolding enthalpy change assigned to forces other than the hydrophobic effect.

The conformational free energies of the metmyoglobins of at least 16 different species (Puett, 1973; Puett et al., 1973; Pace & Vanderburg, 1979; McLendon, 1977; Bismuto et al., 1984; Holladay, 1985, 1986; Kelly & Holladay, 1987, 1990; Kelly et al., 1988) have been estimated at pH 7–8 and 298 K from guanidinium chloride or urea isothermal studies using the binding models developed by Aune and Tanford (1969). The variation in the estimated stability is large, ranging from 68 kJ/mol for rat and rabbit (Kelly et al., 1988) to 26 kJ/mol for armadillo (Kelly & Holladay, 1990). Other species having myoglobins with especially low stabilities are alligator and snapping turtle (Kelly & Holladay, 1987; Puett et al., 1973). Most mammalian metmyoglobins have an estimated conformational free energy of 38–46 kJ/mol (Puett, 1973; Puett et al., 1973; McLendon, 1977; Flanagan et al., 1983; Bismuto et al., 1984; Kelly & Holladay, 1987, 1990; Kelly et al., 1988). The origin and consequences of these varying stabilities have been the subject of much speculation. Several hypotheses have been advanced as to the selection pressures that may have led to the divergence in stabilities (Puett et al., 1973; Goldberg & Dice, 1974; Goldberg & St. John, 1976; McLendon, 1977; Kelly et al., 1988; Kelly & Holladay, 1990). Some comparative studies (Puett, 1973; Flanagan et al., 1983) have suggested that much of the variation in stability arises from differences in polar and salt bond interactions. Calculations based on Baldwin's (1986) hydrophobic model for protein folding suggest that only a small variation in the change in heat capacity can be tolerated without the loss of the predicted stability. A comparison of the available sequence data and the known tertiary structures of sperm whale (Takano, 1977) and horse (Evans & Brayer, 1988) myoglobins shows that the placement of the hydrophobic internal residues, whose exposure to solvent on unfolding is largely responsible for the change in heat capacity, is well conserved over the course of divergent evolution of these two species.

The thermal denaturation of sperm whale metmyoglobin and apomyoglobin has been extensively studied by Privalov and co-workers (Privalov et al., 1971, 1986; Privalov & Khechinashvili, 1974; Privalov, 1979; Griko et al., 1988) at both alkaline and acid pH. The thermal unfolding is largely reversible if the sample is not heated at too high a temperature for too long a time (Griko et al., 1988). The data obtained suggest that the change in enthalpy on unfolding, once ion binding effects are subtracted out, is dependent only on T_d,[1] the temperature at which the unfolding is half-complete, and not on the pH per se. These data also suggest that the change in heat capacity is, within the precision of the data, reasonably

† Supported by NIH DK 40188.
‡ Present address: San Mateo, CA 94403.
§ Present address: Beckman Instruments Co., 1050 Page Mill Rd., Box 10200, Palo Alto, CA 94303-0803.

[1] Abbreviations: T_d, temperature in kelvin at which unfolding is half-complete; DSC, differential scanning calorimetry; ΔC_p, change in heat capacity on unfolding; $C(T)$, excess heat capacity due to the protein; $C_N(T)$, heat capacity of the native protein; Δn_{H^+}, change in number of bound protons on unfolding; ΔH_{cal}, calorimetric enthalpy change; ΔH_{conf}, conformational enthalpy change; Δn_G, change in number of guanidinium ions bound upon unfolding; $D_{1/2}$, concentration of guanidinium chloride at $\Delta G = 0$; ΔH_{obs}, observed enthalpy change; ΔH_{hyd}, change in enthalpy attributable to the hydrophobic effect; ΔH_{res}, defined as $\Delta H_{obs} - \Delta H_{hyd}$; ΔS_{obs}, observed change in entropy; ΔS_{hyd}, change in entropy attributable to the hydrophobic effect; ΔS_{res}, defined as $\Delta S_{obs} - \Delta S_{hyd}$; ΔG_{obs}, observed change in free energy.

0006-2960/90/0429-5062$02.50/0